Quantification of extreme ship response probability in broadband wave fields

Xianliang Gong, Yulin Pan
Department of Naval Architecture and Marine Engineering
University of Michigan, Ann Arbor, MI 48109 USA

1 INTRODUCTION

The evaluation of extreme ship statistics plays a vital role in ship design for at-sea integrity and crew safety. The direct computation (by simulating the ship going through a very long wave field), however, is prohibitively expensive due to the high dimensionality of the random wave field, the rareness of the extreme responses, and the expensiveness of the numerical model. To reduce the computational cost, techniques including wave field parameterization and sequential sampling has been introduced in previous works [1, 2, 3]. These works all assume a narrowband wave spectrum, which enables the representation of the wave field by consecutive Gaussian groups (figure 1(a)). In contrast, the realistic wave fields are mostly broadband, where groups do not necessarily form Gaussian shape (figure 1(b)). In this work, we extend our previous work on temporal exceeding probability [3] to broadband wave fields. A new wave field parameterization and the associated sequential sampling algorithm are developed, followed by a validation case demonstrating the effectiveness of new methodology.

2 METHODOLOGY

We consider a long wave elevation time series $\eta(t), t \in [0, T_{end}]$ generated from a broadband wave spectrum with significant wave height H_s and peak period T_p. Our objective is to evaluate the temporal exceeding probability of ship responses (i.e., the percentage of time that the ship response is larger than a threshold r_s) when a ship goes through the wave field, defined as

$$P_{temp} = \frac{\int_0^{T_{end}} \mathbf{1}\big(|r(t)| - r_s\big)\mathrm{d}t}{T_{end}}, \tag{1}$$

where $r(t)$ is the time series of ship response caused by waves $\eta(t)$ and $\mathbf{1}(\cdot)$ is the indicator function.

When coupled with high-fidelity ship simulations (e.g., CFD), the computational cost of P_{temp} can become prohibitively high. In order to reduce the computational cost, two essential components are developed: a wave group parameterization method to reduce the dimensionality of the wave field and a sequential sampling method to reduce the number of samples (in the low-dimensional parameter space). These two components targeting broadband wave fields are presented next.

2.1 Wave parameterization

Inspired by [4], we define a (dangerous) wave group as a series of consecutive single waves (based on zero-crossing) with amplitudes above a given threshold, here set as $\Delta\eta = H_s/2$ (figure 2 (a)). If groups are too close to each other, i.e., separated by only one wave below the threshold, we will treat them as one group. For example, the second group enclosed in figure 2 (a) is considered as a single group, which contains three continuous waves with two above the threshold and the middle one below the threshold. Each wave group is parameterized by its length l and maximum amplitude a. The collection of all groups provides a two-dimensional parameter space with known probability density function (PDF) $p_{LA}(l, a)$ (figure 2 (b)).

This parameterization significantly reduces the dimension of the wave field, paving the road for a feasible low-dimensional sampling. However, complete neglect of reduced dimensions will lead to an inaccurate result considering the intrinsic high-dimensionality of the broadband wave field.

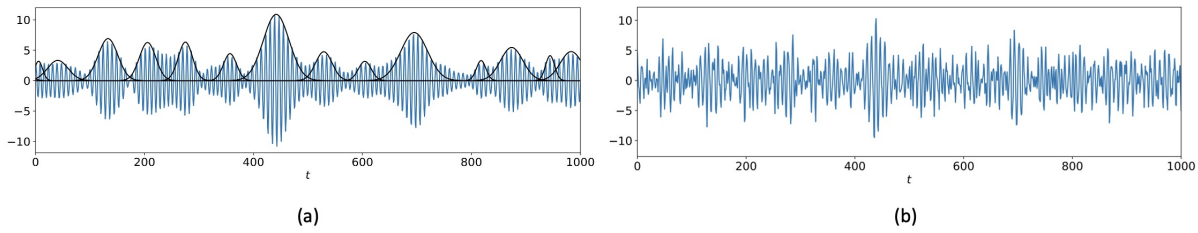

Figure 1: Wave fields generated from (a) narrowband and (b) broadband spectra. The narrowband wave field (a) can be parameterized by Gaussian groups denoted by (—) as in existing work [3], but the broadband wave field (b) contains wave groups that are much less Gaussian-like.

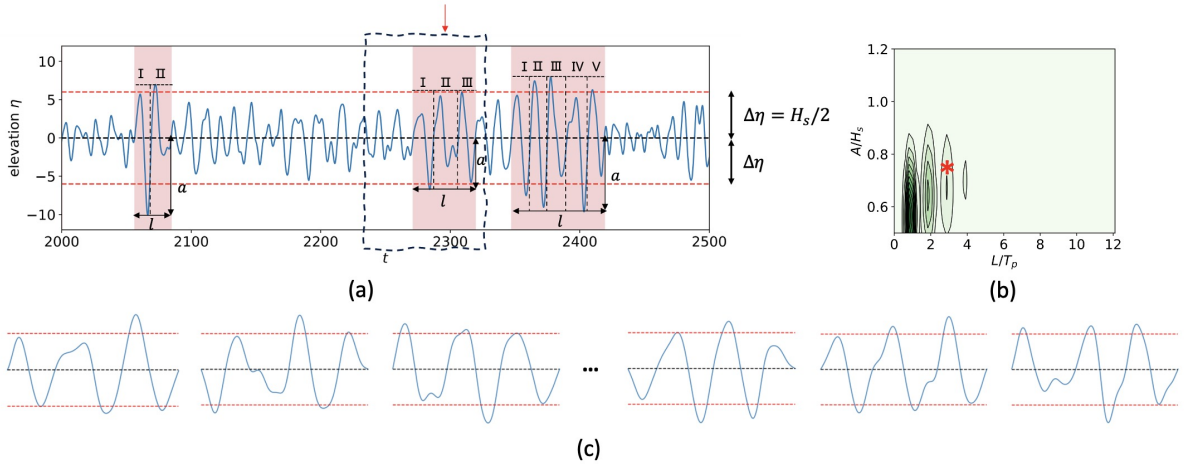

Figure 2: (a) Wave groups (the shaded region) in a broadband wave field. (b) The PDF of the low-dimensional parameter space (L, A), with the two parameters normalized by peak wave period T_p and significant wave height H_s. (c) Six different wave groups with the same parameter ($l = 3T_p, a = 0.75H_s$) ($\star$ in (b)).

For example, groups with the same characteristic length may have significantly different detailed shapes (figure 2 (c)). These different detailed shapes, together with the random initial condition of ship encountering each wave group (denoted jointly by ω), lead to a random exceeding time for groups with the same parameters. Accounting this randomness associated with the low-dimensional parameter space, (1) can be rewritten as:

$$P_{temp} = \frac{m}{T_{end}} \int \mathbb{E}_\omega[S(l, a, \omega)] p_{LA}(l, a) \, \mathrm{d}l\mathrm{d}a, \tag{2}$$

where m is the number of wave groups in $[0, T_{end}]$, $S(l, a, \omega) = \int \mathbf{1}\big(|r(t; l, a, \omega)| - r_s\big)\mathrm{d}t$ is the time of responses $r(t; l, a, \omega)$ exceeding r_s in group (l, a) with randomness ω.

In order to incorporate randomness ω in constructing the function $S(l, a, \omega)$, after a sample (l, a) is chosen, we randomly select a wave group with parameter (l, a) in $\eta(t)$, and simulate ship responses starting from several waves ahead of the selected group (for the pointed group in figure 2 (a), the computational domain is the black dashed window). In this way, we naturally incorporate the randomness from both the detailed wave form and initial responses.

2.2 Sequential sampling

We then design an efficient sequential sampling method based on the Bayesian experimental design

(BED) for the computation of (2) without evaluating of $S(l,a,\omega)$ for all groups. We will next introduce two basic components of this BED: (1) an inexpensive surrogate model to obtain $S(l,a,\omega)$ and (2) an acquisitive function based on which to select the next-best sample sequentially.

We use the Gaussian process regression (GPR) as the surrogate model which provides with both function prediction and uncertainty. However, the direct learning of $S(l,a,\omega)$ by GPR is problematic (see [3] for more details). Instead, we focus on a transformation of S defined as:

$$h(l,a,\omega) = \begin{cases} \dfrac{S(l,a,\omega)}{l}, & if\ S(l,a,\omega) > 0 \\ \dfrac{r_{max}(l,a,\omega) - r_s}{r_s}, & if\ S(l,a,\omega) = 0 \end{cases}, \tag{3}$$

where r_{max} is the maximum response in this group and the second branch in (3) is introduced to ensure that h is a smooth function. To continue, we re-write h as:

$$h(l,a,\omega) = \overline{h}(l,a) + \delta(\omega), \tag{4}$$

where $\overline{h}$ and δ respectively represent the mean and random part of h. In GPR, given a dataset $\mathcal{D} = \{(l^i,a^i), h(l^i,a^i,\omega)\}_{i=1}^{i=n}$ consisting of n inputs and the corresponding outputs, we can approximate (4) as:

$$\overline{h}(l,a)|\mathcal{D} \sim \mathcal{GP}(\mu_h(l,a|\mathcal{D}), \sigma_h^2(l,a|\mathcal{D})), \tag{5}$$

$$\delta(\omega)|\mathcal{D} \sim \mathcal{N}(0, \sigma_0^2|\mathcal{D}), \tag{6}$$

with μ_h and σ_h^2 respectively the posterior mean and variance of $\overline{h}$. The uncertain component $\delta(\omega)$ is approximated as an independent Gaussian with constant variance σ_0^2. We note that a more accurate representation with (l,a)-dependent variance is possible with the heteroscedastic GPR applied in [5].

After the GPR of h is available, we can recover function S by $S \equiv \mathbf{1}(h)\, h\, l$ and compute P_{temp} using (2). Due to the uncertainty in $\overline{h}$, P_{temp} is a random variable with randomness estimated by

$$U|\mathcal{D} = \int \big(\mathbb{E}_\omega[S^+(l,a,\omega)|\ \mathcal{D}] - \mathbb{E}_\omega[S^-(l,a,\omega)|\ \mathcal{D}]\big) p_{LA}(l,a)\ \mathrm{d}l\mathrm{d}a, \tag{7}$$

where $S^\pm(l,a,\omega|\ \mathcal{D}) = \mathbf{1}\big(\mu_h^\pm(l,a) + \delta(\omega)|\ \mathcal{D}\big)\big(\mu_h^\pm(l,a) + \delta(\omega)|\ \mathcal{D}\big) l$ with $\mu_h^\pm = \mu_h \pm \sigma_h$ the upper and lower bounds of $\overline{h}$ prediction. We then select the next sample which is expected to reduce the uncertainty in P_{temp} significantly, i.e., a sample corresponding to the maximum of the integrand in (7):

$$l^*, a^* = \mathrm{argmax}_{l,a}\big(\mathbb{E}_\omega[S^+(l,a,\omega)|\ \mathcal{D}] - \mathbb{E}_\omega[S^-(l,a,\omega)|\ \mathcal{D}]\big) p_{LA}(l,a). \tag{8}$$

This sampling selection procedure will be repeated until the computation budget limit is reached.

3 RESULTS

In this section, we validate the proposed method with ship responses $r(t)$ simulated by a roll equation:

$$\ddot{r} + \alpha_1\dot{r} + \alpha_2\dot{r}|\dot{r}| + (\beta_1 + \epsilon_1\cos(\theta)\eta(t))r + \beta_2 r^3 = \epsilon_2\sin(\theta)\eta(t), \tag{9}$$

which models the ship roll response due to nonlinear resonance and parametric roll in oblique irregular waves. Empirical coefficients are set as $\alpha_1 = 0.35$, $\alpha_2 = 0.06$, $\beta_1 = 0.04$, $\beta_2 = -0.1$,

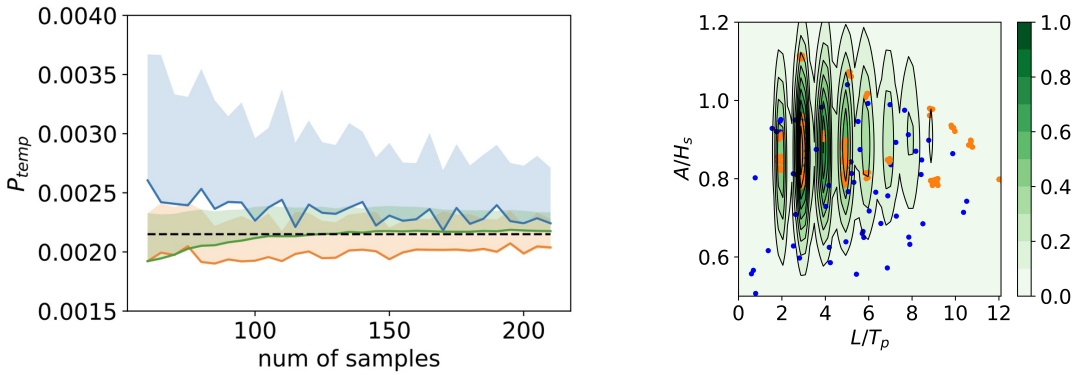

(a) (b)

Figure 3: (a) Results of P_{temp} calculated by random sampling (—), LH sampling (—) and sequential sampling (—) in comparison with ground truth (- - -). The shaded region represents one standard deviation above the mean estimated from 100 applications of each method. (b) Positions of initial samples (●) and sequential samples (●) in the parameter space with a contour plot of $\mathbb{E}_\omega[S(l,a,\omega)]p_{LA}(l,a)$.

$\theta = \pi/6$, $\epsilon_1 = 0.016$, and $\epsilon_2 = 0.012$. The wave field $\eta(t)$ to be parameterized is generated from a JONSWAP spectrum with $H_s = 12m$, $T_p = 15s$, and $\gamma = 3$.

Following procedures in §2, the result of P_{temp} computed by the proposed method for $r_s = 0.3$ is shown in figure 3 (a). For comparison, we also present results from random sampling (by randomly select groups following distribution $P_{LA}(l,a)$), Latin hypercube (LH) sampling (by uniformly covering the parameter space) along with the true solution of P_{temp} (by brute-force calculations for the whole $\eta(t)$ from $t = 0$ to $t = 2.5$ million T_p). The sequential sampling is conducted with an initial data set of 60 LH samples, followed by 150 sequential samples. In order to have a fair comparison, we perform all three sampling methods 100 times starting from different initial samples, and present the mean and stand deviation of the results. It is clear that the sequential sampling result approaches to the true solution of P_{temp} much faster with a smaller uncertainty than those from random and LH samplings.

We further plot the sample positions with the contour of $\mathbb{E}_\omega[S(l,a,\omega)]p_{LA}(l,a)$ in figure 3 (b). We note that $\mathbb{E}_\omega[S(l,a,\omega)]p_{LA}(l,a)$ provides a measure of the importance of groups (l,a) in computing P_{temp}, which can also be seen from (2). As shown in the figure, most sequential samples are driven to the region with significant $\mathbb{E}_\omega[S(l,a,\omega)]p_{LA}(l,a)$, indicating the effectiveness of our BED algorithm.

REFERENCES

[1] Gong, X., Zhang, Z., Maki, K. J., and Pan, Y. 2021. *Full resolution of extreme ship response statistics. arXiv preprint arXiv:2108.03636*.

[2] Mohamad, M. A., and Sapsis, T. P. 2018. *Sequential sampling strategy for extreme event statistics in nonlinear dynamical systems.* Proceedings of the National Academy of Sciences 115(44), 11138–11143.

[3] Gong, X., Siavelis, K., Zhang, Z., and Pan, Y. 2022. *Efficient computation of temporal exceeding probability of ship responses in a random wave field. Applied Ocean Research 129*, 103405.

[4] Bassler, C. C., Belenky, V., and Dipper, M. Application of wave groups to assess ship response in irregular seas. In *Proc. 11th int. ship stability workshop* (2010).

[5] Gong, X., and Pan, Y. 2022. *Sequential Bayesian experimental design for estimation of extreme-event probability in stochastic input-to-response systems. Computer Methods in Applied Mechanics and Engineering 395*, 114979.